Front. Optoelectron. 2017, 10(2): 132–137
DOI 10.1007/s12200-017-0681-0

RESEARCH ARTICLE

Characterization of the cooling process of solid *n*-alkanes via terahertz spectroscopy

Chen JIANG, Honglei ZHAN, Kun ZHAO (✉), Cheng FU

Beijing Key Laboratory of Optical Detection Technology for Oil and Gas, China University of Petroleum, Beijing 102249, China

© Higher Education Press and Springer-Verlag Berlin Heidelberg 2017

Abstract The terahertz (THz) time-domain spectroscopy technique was used to characterize the cooling process of solid *n*-alkanes. The THz waveforms of *n*-octadecane, *n*-nonadecane, *n*-eicosane, *n*-heneicosane, *n*-docosane, and *n*-pentacosane were obtained with the cooling time using the aforementioned noncontact optical method. The peak values of the THz signal were found to be related to the cooling temperature of *n*-alkanes. The THz wave was sensitive to the size and structure of particles in the liquid; therefore, the crystallization process of *n*-alkanes was monitored. An empirical equation based on signal attenuation was proposed to quantitatively distinguish the content change of structural order in the samples. Results present a new noncontact optical approach for characterizing wax crystallization via THz time-domain spectroscopy.

Keywords solid *n*-alkanes, terahertz (THz) time-domain spectroscopy, cooling process

1 Introduction

Crystallization in a solution, particularly wax and asphaltene crystallization in a hydrocarbon system, is a notable phenomenon from the perspectives of both science and technology [1–3]. The precipitation and deposition of wax and asphaltene during the production and transportation of petroleum are common and compatible processes [4–8], which pose considerable challenges to safe and economical operations. Hydrocarbons with a relatively high molecular weight, such as wax and asphaltene in petroleum cuts, as well as their properties, are sensitive to temperature [9,10].

Temperature is related to the structural state, such as the phase transition, of *n*-alkanes [11–13]. Crystal nucleation from a melt is one of the most comprehensively studied phase transition types [14]. *N*-alkanes are important components of crude oil, and their nucleation has been the focus of considerable attention [15–17]. The aforementioned transitions exhibit several unusual features, including the existence of intermediate rotator phases between the liquid and crystalline solid phases and surface freezing prior to solidification [18]. In many phase transitions, the critical dynamical questions involve the vibrational modes of a system, as characterized by the vibrational density of states (VDOS). A peak in low-frequency VDOS is associated with a molecular-scale disorder [19,20]. However, the boson peak that is typically observed over a wide temperature range has not previously been related to a strongly temperature-dependent phenomenon, such as liquid–solid phase transition [21–23].

Recent studies have indicated that terahertz (THz) spectroscopy is a promising method for analyzing hydrocarbon and their mixtures with organic solvents. Al-Douseri et al. presented the performance of THz sensing of gasoline products. They used THz spectroscopy to quantitatively determine xylene isomers in gasoline [24]. The far-infrared spectroscopy of molecules is attaining increasing importance in astrochemistry. Cataldo et al. analyzed 33 polycyclic aromatic hydrocarbons (PAHs) and asphaltenes from petroleum fractions, bitumen, and anthracite coal in THz range [25]. Tian et al. investigated the THz spectral features of liquid alkanes (C_5–C_{10}), and the results suggested that the refractive index of liquid alkanes would increase with increasing carbon number [26]. Liquid alkanes from pentane to hexadecane at temperatures ranging from 20 °C to 80 °C were measured by Laib et al. via THz spectroscopy [21,23]. Zhan et al. proposed an effective method for qualitatively identifying crude oils from different oil fields based on THz time-domain spectroscopy (THz-TDS) [27]. Lubricating oil, which has considerable industrial significance, consists of several types of hydrocarbons. Naftaly et al. focused on the optical absorption properties of oil composition based on THz-TDS [28].

Received December 5, 2016; accepted January 23, 2017

E-mail: zhk@cup.edu.cn

In the present study, THz-TDS was used to measure the temperature-dependent time-domain spectra of six solid *n*-alkanes with carbon numbers ranging from 18 to 25. All the samples were heated to a temperature above the melting point and then naturally cooled. THz spectroscopy for online monitoring provides a new experimental tool for characterizing and evaluating the wax crystallization process. This method also provides a new approach for quantitatively distinguishing the content changes of structural order using the THz-TDS noncontact optical method.

2 Materials and methods

Analytically pure *n*-alkanes were supplied by Aladdin Chemistry (Shanghai) Co., and the carbon numbers of *n*-alkanes were 18, 19, 20, 21, 22, and 25. The purity of the samples is over 99.5%; hence, further purification is unnecessary. The samples are all white powder at room temperature. The diagram of the THz-TDS setup with a sample cell is shown in Fig. 1. A conventional transmission THz-TDS system with a mode-locked titanium: sapphire laser (MaiTai, Spectra Physics) was used in this research. The amplitude and phase information of the samples were obtained simultaneously via THz-TDS based on coherent measurement. THz radiation was generated using an emitter, which was composed of a photoconductive antenna. An optical lens was used to focus THz pulses onto a sample, and then the THz beam that carried the information of the sample encountered the probe laser beam at the zinc telluride crystal in the THz detector. A lock-in amplifier was used to amplify the signal. The THz beam path was purged with nitrogen to minimize the absorption of water vapor. Humidity was maintained at less than 3.0%. A quartz vessel with 1 mm wall thickness and dimensions of 40 mm × 10 mm × 45 mm was selected as the sampler to improve signal-to-noise ratio. The minor absorption of THz waves made the quartz vessel an ideal sampler for THz measurement. The temperature of the samples was controlled using a circulating water–heat exchanger with a temperature resolution of 0.1°C. The samples were heated to 80°C and placed in a THz device. Natural cooling and online monitoring were started via THz-TDS. A thermocouple with an accuracy of 0.1°C was inserted into a sample to monitor temperature. The THz spectra of the reference specimen and the samples were obtained by scanning an empty quartz cell and a quartz cell filled with the sample.

3 Results and discussion

The cooling time-dependent THz waveforms of the six samples are presented in Fig. 2, where the THz signal decreases at different speeds with the increase in cooling

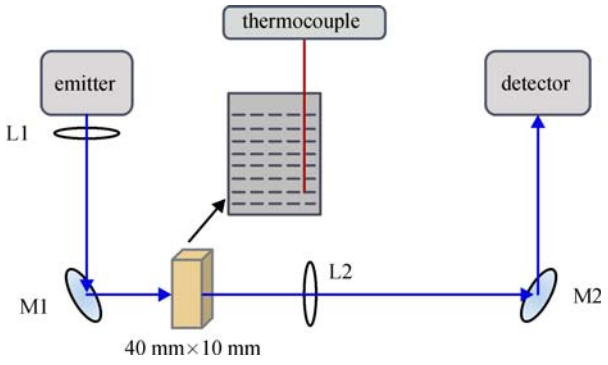

Fig. 1 Diagram of the THz-TDS setup with a sample cell

time. In addition to cell walls, THz waves penetrate hydrocarbons at a fixed path of 8 mm. The THz waveforms of the six samples shown in Figs. 2(a)–2(f) indicate that THz peaks and time delay change with increasing cooling time. The cooling process for the six samples lasts for half an hour. A significant difference among waveforms is observed, thereby suggesting a significant correlation between the different existential states of *n*-alkanes and THz waves. In this study, THz signal intensity and time delay for various *n*-alkanes differ from those of others. The electromagnetic properties of *n*-alkanes in THz range are closely related to chain lengths and structure-dependent properties. The waveform change of *n*-pentaccosane during cooling is the most substantial, followed by those of *n*-docosane, *n*-heneicosane, *n*-eicosane, *n*-nonadecane, and *n*-octadecane. The peak value (E_P) of THz signals depends significantly on cooling time. The peak values (E_P) with cooling time of the six samples shown in Figs. 2(a)–2(f) are presented in Fig. 2(g). In particular, the peak value (E_P) of *n*-pentaccosane changes slightly during the first 4 min. Then, a sharp change in E_p from 0.14831 to 0.02285 V is observed in the succeeding 16 min. The peak value remains nearly unchanged in the last 10 min. The change in peak value is more remarkable for hydrocarbons with a long chain than for those with a short chain.

The temperature decline of over 30 min in the samples is plotted in Fig. 3. The temperature measurements indicate that the cooling rate is sensitive to the chain lengths of *n*-alkanes. For *n*-octadecane, temperature drops abruptly in the first 10 min of cooling. The initial temperature of *n*-octadecane is 52.2°C, and then it drops to 27.2°C after 10 min. However, the temperature decrease of *n*-octadecane is only 1.6°C. To compare the temperature change of the six samples during the same cooling period, the entire cooling process is divided into three stages at every 10 min. As shown in Fig. 3, all the six *n*-alkanes suffer from a dramatic temperature drop in the first 10 min. In the second 10 min, a moderate temperature drop, with a range that is smaller than that of the first part, occurs. For example, the temperature of *n*-docosane changes from 51.5°C to 38.2°C after cooling for 10 min, and the temperature difference

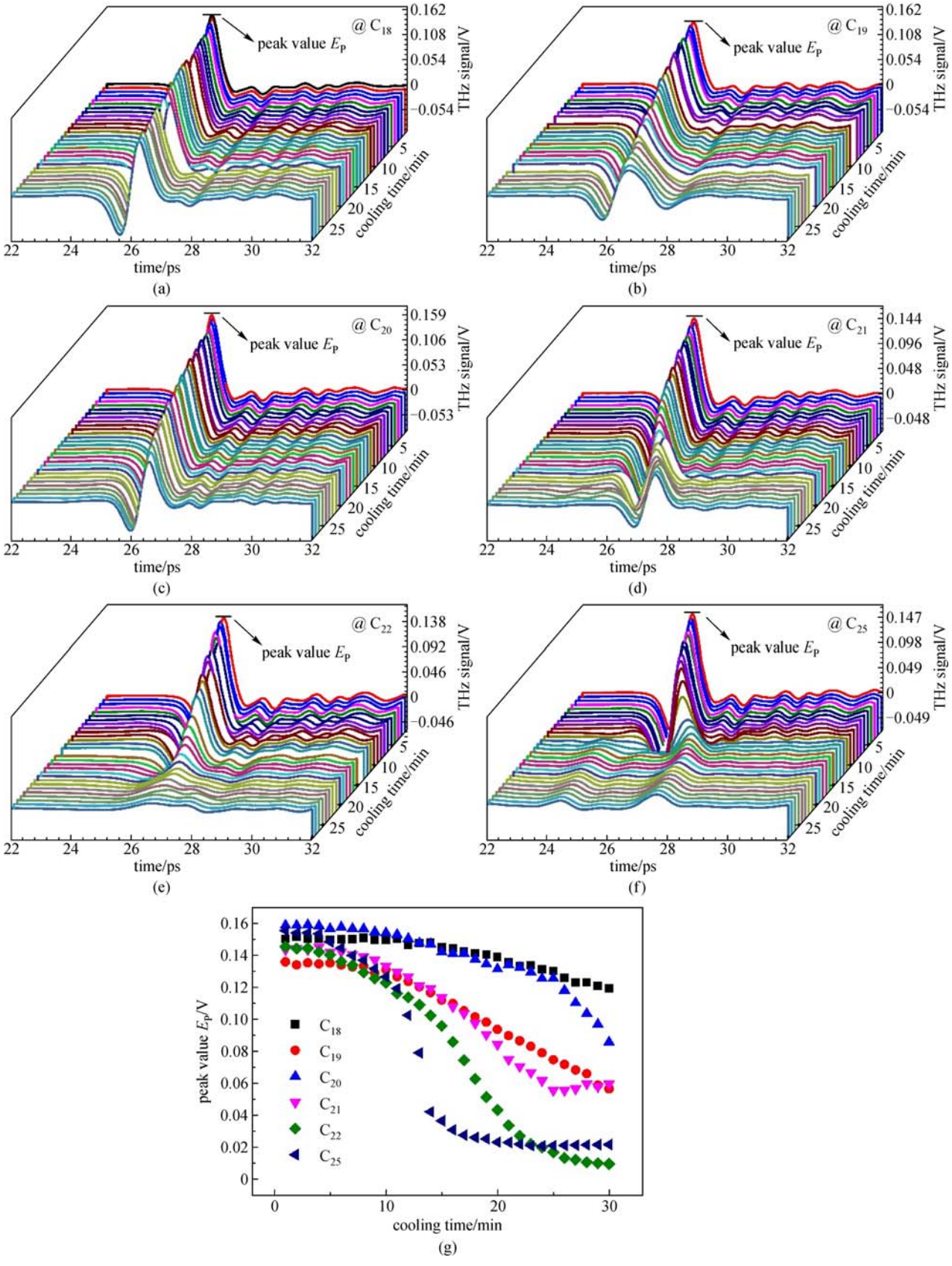

Fig. 2 THz waveforms of cooling time in the samples: (a) *n*-octadecane C_{18}, (b) *n*-nonadecane C_{19}, (c) *n*-eicosane C_{20}, (d) *n*-heneicosane C_{21}, (e) *n*-docosane C_{22}, and (f) *n*-pentaccosane C_{25}. (g) Peak value (E_P) with the cooling time of the six samples

reaches 13.3°C. In the second 10 min, the temperature difference decreases to 5.3°C. During the last 10 min of cooling, the change in temperature of the six *n*-alkanes is scarcely observable. The temperature differences are 0.9°C, 2.1°C, 3.3°C, 2.0°C, 3.3°C, and 5.3°C for $C_{18}H_{38}$, $C_{19}H_{40}$, $C_{20}H_{42}$, $C_{21}H_{44}$, $C_{22}H_{46}$, and $C_{25}H_{52}$, respectively. Consequently, the heat release of the alkanes with a high carbon number accelerates. The variations in peak value and temperature of the samples are considered closely related to the crystallization of *n*-alkanes according to Figs. 2 and 3.

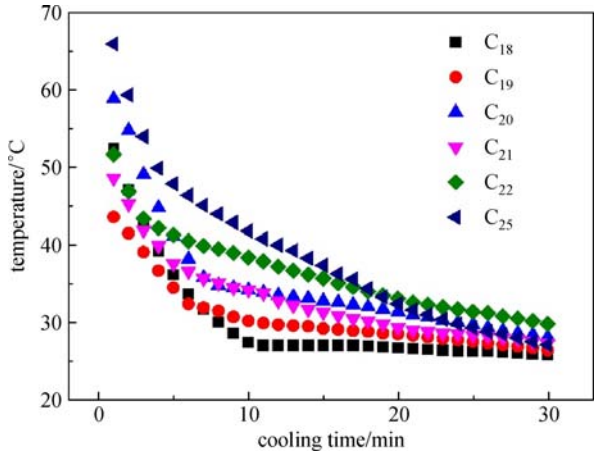

Fig. 3 Temperature variation in the different cooling times of the six samples

Figure 4 is plotted to provide a deeper insight into the variation of the peak value (E_P) with respect to natural cooling. The peak value (E_P) does not exhibit a linear change with the temperature of the samples, thereby indicating that the chain length and existence state of the *n*-alkanes cause the change in peak value. At the beginning

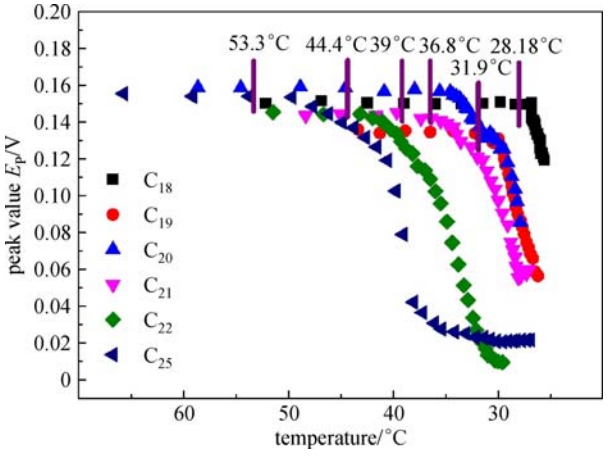

Fig. 4 Peak value (E_P) with the temperature of the six samples. Melting point is 28.18°C, 31.9°C, 36.8°C, 39°C, 44.4°C, and 53.3°C for $C_{18}H_{38}$, $C_{19}H_{40}$, $C_{20}H_{42}$, $C_{21}H_{44}$, $C_{22}H_{46}$, and $C_{25}H_{52}$, respectively

of the THz test, the six samples were melted by heating. When the temperature of the samples is above the melting point, the samples are maintained in liquid state. The lines marked in Fig. 4 show the melting points of each *n*-alkane. The melting points of the alkanes, with their corresponding curves located from right to left in Fig. 4, significantly increase. Crystallization commences when temperature reaches the melting point. Solid and liquid phases coexist before the end of the crystallization process. In addition, the solid fraction in liquid significantly affects the peak values of the samples. The dramatic decline in E_P occurs at a temperature that approaches the melting point because the THz wave is sensitive to the size and structure of the particles in liquid. When the crystallization of the *n*-alkanes starts, a crystal nucleus initially appears in liquid phase; then, the number of crystal nuclei continues to increase. Finally, the *n*-alkanes crystallize thoroughly and become white solid materials. Consequently, significant changes with a sharp slope in E_P are observed, as shown in Fig. 4.

A preliminary exploration of inducing the signal attenuation (SA) equation is conducted by combining the experimental results of the THz tests and the exothermic test to estimate the cooling process as follows:

$$\mathrm{SA} = |E_P^2/E_{P0}^2| \times 100\%,$$

where E_P is the peak value of the THz signal for the sample measured at any time during the cooling period, and E_{P0} is the peak value of the THz signal for the same sample measured prior to cooling. The temperature-governed SA shown in Fig. 5 identifies the phase-based change in the cooling process. Such SA model is adopted to numerically distinguish structural change in the alkane samples to the maximum extent. For the cases in which SA is nearly 100%, the sample is considered in the state of complete disorder, whereas for the cases in which SA is approximately 0%, the state of the sample is considered in order. As shown in Fig. 5, liquid samples exist within a

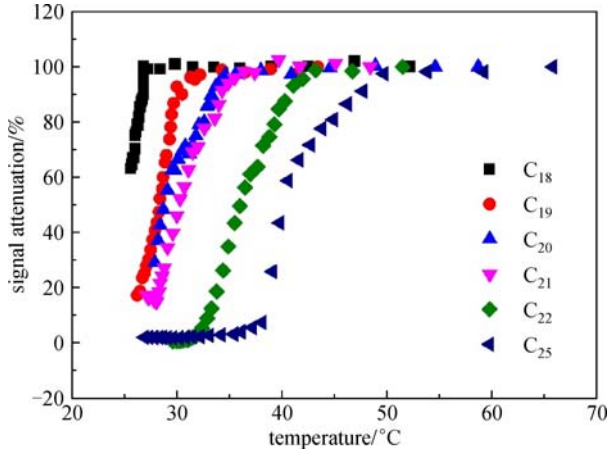

Fig. 5 Temperature-governed signal attenuation for the six samples

temperature range that exceeds the melting point, and accordingly, SA is ~100%. As temperature drops, the liquid sample changes into solid, accompanied by the recovery of molecular order and the increase in SA value. Thus, the SA value is small for solid samples. The melting points are 28.18°C, 31.9°C, 36.8°C, 39°C, 44.4°C, and 53.3°C for $C_{18}H_{38}$, $C_{19}H_{40}$, $C_{20}H_{42}$, $C_{21}H_{44}$, $C_{22}H_{46}$, and $C_{25}H_{52}$, respectively. At the same cooling time, the final temperatures reach 25.6°C, 26.2°C, 27.9°C, 27.1°C, 29.6°C, and 26.9°C, respectively. In addition, ΔT is defined as the difference between the melting point and the final temperature. Figure 5 also indicates that not all the sample curves reach 0% because of the limited temperature range monitored via THz-TDS. For example, when SA is ~0% for $C_{25}H_{52}$, ΔT reaches 26.4°C and becomes sufficiently high to achieve perfect crystallization. The exothermic process slows down because of the small ΔT (2.58°C) for $C_{18}H_{38}$. Only some parts of the liquid sample have changed into solid, and therefore, the SA value does not reach 0%.

Gaber and Peticolas proposed a parameter to describe the degree of lateral inter-chain order and localized intra-chain conformational order based on Raman spectral intensity [29]. On the basis of previous works, information, such as the intensity of Raman spectroscopy, is obtained for the quantitative analysis of the phase transition process of alkanes. Octane, dodecane, and hexadecane were used as models to describe portions of the Raman spectrum of PE, and the effect of conformation on the spectral intensities was studied [30–32]. Meier's theory states that the definition of order parameter fails to provide a precise description of the change in the amount of ordered fraction within alkane samples and only provides the relative amount of ordered fraction [33].

The cooling of *n*-alkanes is regarded as an extremely complicated process accompanied by a variety of complex phase changes. A number of factors work on peak values. In this study, SA is measured and analyzed qualitatively. However, the mechanism is inexplicit and a detailed research is necessary in the future. The SA empirical equation obtained in this research, which targets six types of alkane, also requires correction. Nevertheless, the proposed THz-TDS technology provides a novel method for characterizing change in structural order that is applicable to evaluating wax crystallization.

4 Conclusions

In this work, THz-TDS was used to monitor phase change, particularly the crystallization, of six types of *n*-alkanes. The peak values of the THz signal were found to be associated with the cooling temperature of *n*-alkanes because the THz wave was sensitive to the size and structure of the particles in a liquid. In addition, an empirical equation based on SA was proposed to describe the extent to which molecular structural order changes numerically. The present study suggests a novel non-contact optical method for characterizing the crystallization of wax using THz-TDS.

Acknowledgements This work was supported by the National Basic Research Program of China (No. 2014CB744302), the Specially Funded Program on National Key Scientific Instruments and Equipment Development (No. 2012YQ140005), the China Petroleum and Chemical Industry Association Science and Technology Guidance Program (No. 20160107), and the National Natural Science Foundation of China (Grant No. 11574401).

References

1. Sirota E B. Supercooling and transient phase induced nucleation in *n*-alkane solutions. Journal of Chemical Physics, 2000, 112(1): 492–500
2. Xie B Q, Liu G M, Jiang S C, Zhao Y, Wang D J. Crystallization behaviors of *n*-octadecane in confined space: crossover of rotator phase from transient to metastable induced by surface freezing. Journal of Physical Chemistry B, 2008, 112(42): 13310–13315
3. Sirota E B. Supercooling, nucleation, rotator phase, and surface crystallization of *n*-alkane melts. Langmuir, 1998, 14(11): 3133–3136
4. Yang X L, Kilpatrick P. Asphaltenes and waxs do not interact synergistically and coprecipitate in solid organic deposits. Energy & Fuels, 2005, 19(4): 1360–1375
5. Visintin R F G, Lockhart T P, Lapasin R, D'Antona P. Structure of waxy crude oil emulsion gels. Journal of Non-Newtonian Fluid Mechanics, 2008, 149(1-3): 34–39
6. Venkatesan R, Nagarajan N R, Paso K, Yi Y B, Sastry A M, Fogler H S. The strength of paraffin gels formed under static and flow conditions. Chemical Engineering Science, 2005, 60(13): 3587–3598
7. Agarwal K M, Purohit R C, Surianarayanan M, Joshi G C, Krishna R. Influence of waxes on the flow properties of Bombay high crude. Fuel, 1989, 68(7): 937–939
8. Rønningsen H P, Bjørndal B, Hansen A B, Pedersen W B. Wax precipitation from north sea crude oils.1. crystallization and dissolution temperatures, and Newtonian and non-Newtonian flow properties. Energy & Fuels, 1991, 5(6): 895–908
9. Briard A J, Bouroukba M, Petitjean D, Hubert N, Moise J C, Dirand M. Thermodynamic and structural analyses and mechanisms of the crystallization of multi-alkane model mixtures similar to petroleum cuts. Fuel, 2006, 85(5-6): 764–777
10. Petitjean D, Schmitt J F, Fiorani J M, Laine V, Bouroukba M, Dirand M, Cunat C. Some temperature-sensitive properties of pure linear alkanes and *n*-ary mixture. Fuel, 2006, 85(10-11): 1323–1328
11. Wang S L, Tozaki K I, Hayashi H, Hosaka S, Inaba H. Observation of multiple phase transitions in *n*-$C_{22}H_{46}$ using a high resolution and super-sensitive DSC. Thermochimica Acta, 2003, 408(1-2): 31–38
12. Tozaki K I, Inaba H, Hayashi H, Quan C, Nemoto N, Kimura T. Phase transitions of *n*-$C_{32}H_{66}$ measured by means of high resolution and super-sensitive DSC. Thermochimica Acta, 2003, 397(1-2): 155–161

13. Wang S L, Tozaki K I, Hayashi H, Inaba H, Yamamoto H. Observation of multiple phase transitions in some even *n*-alkanes using a high resolution and super-sensitive DSC. Thermochimica Acta, 2006, 448(2): 73–81
14. Sirota E B, Herhold A B. Transient phase-induced nucleation. Science, 1999, 283(5401): 529–532
15. Dirand M, Chevallier V, Provost E, Bouroukba M, Petitjean D. Multicomponent paraffin waxes and petroleum solid deposits: structural and thermodynamic state. Fuel, 1998, 77(12): 1253–1260
16. Sirota E B, Herhold A B. Transient rotator phase induced nucleation in *n*-alkane melts. Polymer, 2000, 41(25): 8781–8789
17. Zheng M J, Du W M. Phase behavior, conformations, thermodynamic properties, and molecular motion of multicomponent paraffin waxes: a roman spectroscopy study. Vibrational Spectroscopy, 2006, 40(2): 219–224
18. Shinohara Y, Kawasaki N, Ueno S, Kobayashi I, Nakajima M, Amemiya Y. Observation of the transient rotator phase of *n*-hexadecane in emulsified droplets with time-resolved tow-dimensional small- and wide-angle X-Ray scattering. Physical Review Letters, 2005, 94(9): 097801
19. Grigera T S, Martin-Mayor V, Parisi G, Verrocchio P. Phonon interpretation of the 'boson peak' in supercooled liquids. Nature, 2003, 422(6929): 289–292
20. Shintani H, Tanaka H. Universal link between the boson peak and transverse phonons in glass. Nature Materials, 2008, 7(11): 870–877
21. Laib J P, Nickel D V, Mittleman D M. Terahertz vibrational modes induced by heterogeneous nucleation in *n*-alkanes. Chemical Physics Letters, 2010, 493(4-6): 279–282
22. Zeitler J A, Newnham D A, Taday P F, Threlfall T L, Lancaster R W, Berg R W, Strachan C J, Pepper M, Gordon K C, Rades T. Characteristics of temperature-induced phase transitions in five polymorphic forms of sulfathiazole by terahertz pulsed spectroscopy and differential scanning calorimetry. Journal of Pharmaceutical Sciences, 2006, 95(11): 2486–2498
23. Laib J P, Mittleman D M. Temperature-dependent terahertz spectroscopy of liquid *n*-alkanes. Journal of Infrared, Millimeter and Terahertz Waves, 2010, 31(9): 1015–1021
24. Al-Douseri F M, Chen Y Q, Zhang X C. THz wave sensing for petroleum industrial applications. International Journal of Infrared and Millimeter Waves, 2006, 27(4): 481–503
25. Cataldo F, Angelini G, Aníbal García-Hernández D, Manchado A. Far infrared (terahertz) spectroscopy of a series of polycyclic aromatic hydrocarbons and application to structure interpretation of asphaltenes and related compounds. Spectrochimica Acta Part A: Molecular and Biomolecular Spectroscopy, 2013, 111: 68–79
26. Tian L, Zhou Q L, Zhao K, Shi Y L, Zhao D M, Zhao S Q, Zhao H, Bao R M, Zhu S M, Miao Q, Zhang C L. Consistency-dependent optical properties of lubricating grease studied by terahertz spectroscopy. Chinese Physics B, 2011, 20(1): 010703
27. Zhan H L, Wu S X, Bao R M, Ge L N, Zhao K. Qualitative identification of crude oils from different oil fields using terahertz time-domain spectroscopy. Fuel, 2015, 143: 189–193
28. Naftaly M, Foulds A P, Miles R E, Davies A G. Terahertz transmission spectroscopy of nonpolar materials and relationship with composition and properties. International Journal of Infrared and Millimeter Waves, 2005, 26(1): 55–64
29. Gaber B P, Peticolas W L. On the quantitative interpretation of biomembrane structure by Raman spectroscopy. Biochimica et Biophysica Acta, 1977, 465(2): 260–274
30. Tarazona A, Koglin E, Coussens B B, Meier R J. Conformational dependence of Raman frequencies and intensities in alkanes and polyethylene. Vibrational Spectroscopy, 1997, 14(2): 159–170
31. Meier R J. Corrigendum to "Conformational dependence of vibrational frequencies and intensities in alkanes and polyethylene" by Tarazona et al (Vib. Spectrosc. 14 (1997) 159–170). Vibrational Spectroscopy, 1997, 15(1): 147
32. Koglin E, Meier R J. Conformational dependence of Raman frequencies and intensities in alkanes and polyethylene. Computational and Theoretical Polymer Science, 1999, 9(3-4): 327–333
33. Meier R J, Csiszár A, Klumpp E. Detecting the effect of very low amounts of penetrants in lipid bilayers using Raman spectroscopy. The Journal of Physical Chemistry Letters B, 2006, 110(42): 20727–20728

Chen Jiang obtained her B.Sc. degree from Hebei Normal University of Science and Technology in 2012. She is currently working toward a Ph.D. degree in Materials Science and Engineering at China University of Petroleum, Beijing, China. Her research interest includes terahertz detection of crude oil.

Honglei Zhan obtained his B.Sc. degree from Xiamen University in 2012. He is currently working toward a Ph.D. degree in Materials Science and Engineering at China University of Petroleum, Beijing, China. His research interest includes nano-petrophysics and terahertz metrology.

Kun Zhao obtained his B.Sc. degree in Physics from Nanjing University in 1992, his master's degree from the Institute of Physics, Chinese Academy of Sciences in 1997, and his Ph.D. degree from the Chinese University of Hong Kong in 2001. He is currently a professor in optical engineering and the head of the Beijing Key Laboratory of Optical Detection Technology for Oil and Gas. His research interest includes oil and gas optics.

Cheng Fu obtained her B.Sc. degree from Yangtze University in 2011 and her master's degree from China University of Petroleum, Beijing, China, in 2014. Her research interest includes the application of terahertz spectroscopy in crude oil.